

Complex dynamics approach to Dynamical quantum phase transitions: the Potts model

Somendra M. Bhattacharjee*

Department of Physics, Ashoka University, Sonapat, Haryana - 131029, India

(Dated: March 14, 2024)

This paper introduces complex dynamics methods to study dynamical quantum phase transitions in the one- and two-dimensional quantum 3-state Potts model. The quench involves switching off an infinite transverse field. The time-dependent Loschmidt echo is evaluated by an exact renormalization group (RG) transformation in the complex plane where the thermal Boltzmann factor is along the positive real axis, and the quantum time evolution is along the unit circle. One of the characteristics of the complex dynamics constituted by repeated applications of RG is the Julia set, which determines the phase transitions. We show that special boundary conditions can alter the nature of the transitions, and verify the claim for the one-dimensional system by transfer matrix calculations. In two dimensions, there are alternating symmetry-breaking and restoring transitions, both of which are first-order, despite the criticality of the Curie point. In addition, there are finer structures because of the fractal nature of the Julia set. Our approach can be extended to multi-variable problems, higher dimensions, and approximate RG transformations expressed as rational functions.

I. INTRODUCTION

A dynamical quantum phase transition (DQPT) is a sudden or non-analytic change in the behaviour of a large quantum system during its time evolution. A typical example is the Loschmidt echo, which measures the probability $P(t)$ of finding the system in the original state ψ_0 after time t [1, 2]. Interestingly, these transitions occur at critical times without having to change any of the system's parameters.

Quench dynamics in quantum systems is a widely researched topic that holds importance in several areas. It ranges from conceptual issues such as dynamics in many-body systems, thermalization, entanglements, and novel dynamics to practical applications in quantum computations and information [3–5]. While DQPT was originally observed in the transverse field Ising model [6, 7], subsequent investigations have been conducted on various types of systems for both pure and mixed states [8–15]. Different types of quenches have been studied in Floquet systems, topological models, bosonic and fermionic systems, and many others [16–27]. A crucial question that arises is whether the phases, transitions, or criticalities in DQPT are just analogous to the known thermal phases and transitions observed in the same system or *new phases or transitions may emerge in the quantum domain*.

The terminology used here follows thermodynamic definitions. A system is deemed to be in the same phase at two different times if its properties evolve smoothly whereas a transition between phases happens when the pattern of evolution experiences abrupt or divergent changes in time derivatives [28]. DQPT is classified as a first-order transition if the first derivative of $P(t)$ (or rather, $-\ln P(t)$) in time is discontinuous at the transi-

tion point. Any other form of singular behavior is regarded as a continuous transition.

A. On DQPT

Consider the time evolution of a quantum system described by the Hamiltonian H when started in a state $|\psi_0\rangle$, which is not an eigenstate of H . The state at time t is $|\psi_t\rangle = e^{-iHt}|\psi_0\rangle$ (take $\hbar = 1$). The quantity of interest is the probability of finding the system in the initial state, called the Loschmidt echo, and it is given by

$$P(t) = |L(t)|^2, \quad \text{where } L(t) = \langle \psi_0 | \psi_t \rangle. \quad (1)$$

In the basis of \mathcal{W} orthonormal eigenstates of H ,

$$H = \sum_{n=1}^{\mathcal{W}} E_n |n\rangle \langle n|, \quad (2)$$

with $\langle n | m \rangle = \delta_{nm}$, where δ_{nm} is the Kronecker-delta, the states at time $t = 0$ and t are, respectively,

$$|\psi_0\rangle = \sum_{n=1}^{\mathcal{W}} c_n |n\rangle, \quad \text{and } |\psi_t\rangle = \sum_{n=1}^{\mathcal{W}} c_n e^{-iE_n t} |n\rangle, \quad (3a)$$

so that

$$L(t) = \sum_{n=1}^{\mathcal{W}} |c_n|^2 e^{-iE_n t}, \quad (3b)$$

with $|c_n|^2$ as the probability of the n th state at $t = 0$.

Let us restrict ourselves to the case with $c_n = 1/\sqrt{\mathcal{W}}$, i.e., all eigenstates are equally probable in the initial state. The Loschmidt amplitude is then $L(t) = \frac{1}{\mathcal{W}} \sum_{n=1}^{\mathcal{W}} e^{-iE_n t}$ which is to be compared with the partition function at the inverse temperature β , $Z(\beta) = \sum_n e^{-\beta E_n}$.

* somendra.bhattacharjee@ashoka.edu.in

We define a complex function

$$\mathcal{L}(z) = \frac{1}{\mathcal{W}} \sum_{n=1}^{\mathcal{W}} e^{-zE_n}, \quad (4a)$$

such that

$$\mathcal{L}(z) = \begin{cases} \frac{1}{\mathcal{W}} Z(\beta), & \text{for } z = \beta \text{ (real),} \\ L(t), & \text{for } z = it \text{ (real } t\text{).} \end{cases} \quad (4b)$$

In simpler terms, $\mathcal{L}(z)$ is the extension of the thermal partition function of a quantum system from the real axis to the complex plane by extending the real inverse temperature β to the complex variable z . This analytic continuation connects the partition function to the Loschmidt amplitude.

The extensivity of thermodynamic quantities requires that the free energy $\beta F = -\ln Z$ is proportional to the size of the system so that for N degrees of freedom, $N^{-1} \ln Z$ in the limit $N \rightarrow \infty$ should be independent of N . As an analytic continuation, we then expect $N^{-1} \ln L$ to be also independent of N so that (Re is real part)

$$P(t) = e^{-2Nf}, \text{ where } f = -\text{Re} \lim_{N \rightarrow \infty} N^{-1} \ln L, \quad (5)$$

where f is independent of N , and is called the rate function in the large-deviation theory [29]. The phase transitions are given by the singularities of f .

It is convenient to use $y = e^{\beta\Delta}$ (a Boltzmann factor with $e^{it\Delta}$ as its complex extension) as the variable, instead of β and t , and treat L, Z, \mathcal{L} as functions of y . Here, $\Delta > 0$ is a typical energy scale for the problem. In the complex- y plane, the thermal partition function is defined along the positive real axis while the quantum time evolution is along the unit circle $|y| = 1$. Specifically, the singularities in f as y varies on the unit circle are the DQPTs during the quantum evolution.

B. Objectives

We can use the mathematical approach of zeros of the partition function $Z(y)$ in the complex- y plane to generate the singularities in free energy [30, 31]. It is important to note that, in any finite system, there are no real positive zeros of $Z(y)$ (no phase transition). However, in the thermodynamic limit (infinite size), the zeros may pinch the real axis as a limit point, creating a thermal phase transition. Additionally, the same set of zeros also describes $\mathcal{L}(y)$ (and, so, $L(y)$). Therefore, the local dispositions of the zeros (not just pinching at a point) around the unit circle $|y| = 1$ determine the singularities in $f(y)$ for the Loschmidt echo, connecting the complex zeros to DQPT. A thermodynamic limit is required to ensure a dense set of zeros, without which there can be no phase transitions.

A different but more general framework for analyzing a many-body interacting system is the renormalization

group (RG) method [30, 32], which is the method of choice for DQPT. The technique involves two essential steps. Firstly, small-scale degrees of freedom (df) are integrated out, and their effects are accounted for by adjusting (renormalizing) the effective interactions of the remaining dfs. Secondly, the remaining system is rescaled to keep physical quantities invariant, like the free energy per df. This leads to the transformation of parameters, where y becomes $y' = R(y)$, and the concerned physical quantity is renormalized. By repeatedly performing these steps, the large-scale behavior of the system can be determined by observing how the renormalized parameters approach their fixed point values. The stable fixed points represent the phases of the system, while the unstable ones represent phase transitions or critical points. Apart from these, the renormalization of the free energy allows us to generate the zeros of the partition function in the thermodynamic limit.

This paper explores the relationship between DQPT and the transitions in the equilibrium thermal problem to uncover the possibilities of new phases and transitions. The connection is via the RG transformation in the complex plane and the complex zeros of the partition function in a *class of models amenable to exact analysis*. We study the 3-state Potts model [10, 33–36] defined on hierarchical lattices for which the real-space renormalization group can be implemented exactly, thereby avoiding artifacts of approximations [37–39]. The repeated RG transformations constitute an *iterated map in the complex plane* of a properly defined Boltzmann factor. Results of the dynamics of one complex variable [40–42] (complex dynamics in short) can be made to bear upon the quantum problem. Near-exact numerical computations then supplement these analytical results.

C. Outline

The 3-state quantum Potts model on a lattice is defined in Section II, where the eigenstates and eigenvalues required for the subsequent analysis can be found. The hierarchical lattices used in this paper and their characteristics are in Section II A. The particular quench of interest here is elaborated in Sec. II B while the early time behaviour of the rate function for the Loschmidt echo after the quench is analyzed in Sec. III.

The details of the RG procedure is discussed in Sec. IV. The exact implementation of the RG transformation allows us to compute the rate function as a sum along the RG trajectory, given by Eq. (20c). In this process, a boundary-dependent term emerges that plays a critical role in the one-dimensional case.

The methods of complex dynamics for iterated maps in the complex plane are summarized in Sec. V. The phases and the phase transitions in the system are determined by the flows in the complex plane, which fall into two categories: the Fatou set, controlled by attractive fixed points and the Julia set forming the boundary of the

Fatou set. The properties of these sets are summarized in Sec. V. The Julia set is linked to the zeros of the partition function and the rate function in Sec. VI.

DQPT in the one-dimensional Potts model is discussed in detail, particularly the role of the Julia set, in Sec. VII. We also examine the effects of boundary conditions (Sec. VII A-D) and further corroborate them using a transfer matrix approach (Sec. VII E). In Section VII D 2, we provide a statement on the conditions under which boundaries may suppress an otherwise allowed DQPT. Moving on to the two-dimensional case in Section VIII, we observe that, despite the complications introduced by the wide intersections of the unit circle with the Julia set, DQPTs are first-order and described by the repulsive fixed points of the Julia set. The paper concludes in Sec. IX with a summary and remarks on possible generalizations of the approach developed in the paper.

A few algebraic details can be found in the Appendices. A few periodic orbits for the one-dimensional Potts chain with their multiplicities are listed in Appendix C. The full Julia set for the two-dimensional case is shown in Appendix D.

II. THE POTTS MODEL

We study the three-state ($q = 3$) Potts model on a lattice (Fig. 1) with nearest-neighbour interaction [33–36]. In the quantum model, each site has a Potts variable with eigenstates represented by a planar spin oriented in three symmetric directions: $0, 2\pi/3, 4\pi/3$ on a circle (Fig. 1c). The ferromagnetic interaction generates a three-fold degenerate ground state, which may endure quantum and thermal fluctuations to produce an ordered state. As a result, the model may demonstrate a symmetry-breaking transition (breaking of the discrete permutation symmetry in this case).

The Hamiltonian \mathcal{H} has two parts, (i) an interaction term H that tries to order the spins, and (ii) a ‘transverse-field’ term H_Γ that disrupts ordering by flipping the spins, and these are given by [34]

$$\mathcal{H} = H + H_\Gamma, \quad (6a)$$

$$H = -\frac{\mathcal{J}}{2} \sum_{\langle jk \rangle} (\Omega_j^\dagger \Omega_k + \Omega_k^\dagger \Omega_j), \quad (\mathcal{J} > 0), \quad (6b)$$

$$H_\Gamma = -\Gamma \sum_j \mathbf{T}_j, \quad (6c)$$

where dagger denotes Hermitian conjugate, j, k denote the lattice sites with $\langle \dots \rangle$ denoting nearest-neighbours,

$$\Omega_j = \mathbf{I} \otimes \mathbf{I} \otimes \dots \overset{j\text{th}}{\underbrace{\Omega}} \otimes \mathbf{I} \otimes \dots, \quad (6d)$$

$$\mathbf{T}_j = \mathbf{I} \otimes \mathbf{I} \otimes \dots \underbrace{\mathbf{T}} \otimes \mathbf{I} \otimes \dots, \quad (6e)$$

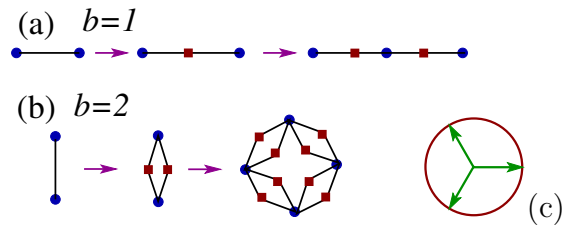


FIG. 1. Hierarchical lattices constructed by replacing a bond by a motif ad infinitum. Here the motif is a diamond of b branches, with each branch adding a new point (red square). Each motif adds $2b$ bonds. Successive lattices are indexed by the generation number n with $n = 0$ for the starting bond. (a) A one dimensional lattice generated by a $b = 1$ ‘diamond’ (which is a line). (b) For $b = 2$, two new sites and $2b = 4$ bonds are created for each bond. Eventually, one gets a 2-dimensional lattice, though not a Bravais lattice. Three generations are shown in (a) and (b). (c) A planar vector representation of a Potts spin with $q = 3$ states. The vectors are mutually at an angle of $2\pi/3$

with Ω, \mathbf{T} at the j th position in the direct products over sites, and \mathbf{I} the identity. The Potts variables are given by ($\omega = e^{i2\pi/3}$)

$$\Omega = \begin{pmatrix} 1 & 0 & 0 \\ 0 & \omega & 0 \\ 0 & 0 & \omega^2 \end{pmatrix}, \quad \text{and } \mathbf{M} = \begin{pmatrix} 0 & 1 & 0 \\ 0 & 0 & 1 \\ 1 & 0 & 0 \end{pmatrix}, \quad (7)$$

with $\mathbf{T} = \mathbf{M} + \mathbf{M}^\dagger$. Here, Ω, \mathbf{T} for the Potts spins are expressed in the eigenstates $|1\rangle, |2\rangle, |3\rangle$, and, in that basis, \mathbf{M} is a spin flip operator, satisfying

$$\Omega^q = \mathbf{M}^q = \mathbf{I}, \quad \text{with } q = 3. \quad (8)$$

The eigenstate for the largest eigenvalue of \mathbf{T} is

$$|0\rangle = \frac{1}{\sqrt{3}}(|1\rangle + |2\rangle + |3\rangle).$$

The special property of \mathbf{T} is that it flips any of the three states $|\mu\rangle, \mu = 1, 2, 3$ to an equal superposition of the other two states, e.g.,

$$\mathbf{T}|1\rangle = |2\rangle + |3\rangle, \quad (9)$$

The 3^N eigenstates of H for N spins, $H|n\rangle = E_n|n\rangle$, are the direct product states of individual spin states $|\alpha\rangle, \alpha = 1, 2, 3$ as

$$|n\rangle = \otimes_j |\alpha\rangle_j \equiv |\alpha_1 \alpha_2 \dots \alpha_N\rangle, \quad (10a)$$

with eigen-values E_n given by

$$E_n = -\mathcal{J} \sum_{\langle jk \rangle} \cos(\theta_j - \theta_k), \quad \theta_j = \frac{2\pi}{3}(\alpha_j - 1). \quad (10b)$$

The ground state for a single pair of spins is a state with parallel spins, $\theta_j = \theta_k$, and has energy $-\mathcal{J}$. This state is threefold degenerate. On the other hand, the excited state is six-fold degenerate and is achieved through

nonparallel spins with $|\theta_j - \theta_k| = 2\pi/3 \pmod{2\pi}$, with an energy of $-J/2$. To simplify our calculation, we shift and rescale the energy to express it as

$$E_n = -J \sum_{\langle jk \rangle} \delta_{\alpha_j, \alpha_k}, \quad (11)$$

so that the ground state energy is $-J$ and the gap in the spectrum for a bond is J . The Boltzmann factor

$$y = e^{\beta J}, \quad (12)$$

appears as the variable of choice.

A. Hierarchical lattices

The Potts spins are placed on the sites of a lattice constructed in a manifestly scale-invariant way, as shown in Fig. 1. The nearest neighbours are defined by the bonds. We start with a single bond with two sites as generation $n = 0$ and a diamond-like motif of $2b$ branches (Fig. 1b) [43]. The lattice for generation n can be constructed from the $(n-1)$ -generation lattice by replacing each bond with the diamond motif. When $b = 1$, the recursive process results in a one-dimensional lattice (Fig. 1a). From the growth of the lattice (the number of bonds B with generation n), the Hausdorff dimension [44] of the lattice is $d_b = \frac{\ln 2b}{\ln 2}$. This expression gives $d_1 = 1$, which is consistent with Fig. 1a, and $d_2 = 2$ for $b = 2$. We consider these two cases, viz., one-dimensional ($b = 1$) and the two-dimensional ($b = 2$) lattices.

The numbers of bonds and sites for generation n are

$$B_n = (2b)^n, \text{ and } N_n = 2 + b \frac{(2b)^n - 1}{2b - 1}, \quad (13)$$

with $\lim_{n \rightarrow \infty} \frac{N_n}{B_n} = \frac{b}{2b-1}$. Thanks to this asymptotic proportionality, we use the number of bonds (instead of the number of spins) to describe extensivity.

The recursive construction of the lattice allows one to implement real-space RG exactly on these lattices [37, 38]. Moreover, dimensionality can be tuned by adjusting the value of b , which allows for a comprehensive examination of the impact of dimensionality on relevant properties. Recent studies have predominantly focused on quantum phase transitions in higher dimensional (> 1) Euclidean lattices for the q -state quantum Potts model [35, 36]. Although mapping the d -dimensional quantum problem to a $(d+1)$ -dimensional classical statistical mechanical problem has proven advantageous, such mappings are of limited use for the hierarchical lattices.

B. The quench and the echo

We are interested in the sudden quench from $\Gamma \rightarrow \infty$ to $\Gamma = 0$. A large field, $\Gamma \rightarrow \infty$, forces the spins to be

in the eigenstate of \mathbf{T} with the largest eigenvalue. This pure state is in a product form

$$|\psi_0\rangle = \bigotimes_j |0\rangle_j = \bigotimes_j \left[\frac{1}{\sqrt{3}} (|1\rangle + |2\rangle + |3\rangle) \right]_j. \quad (14)$$

At time $t = 0$, Γ is switched off, and the Potts system undergoes a unitary evolution with H , Eq. (6b). Our aim is to determine the behaviour of $\mathcal{L}(y)$ (Eq. (4a) and $f(y)$ defined in Eq. (5), by extending the Boltzmann factor to a complex number

$$y = \exp(zJ), \text{ with } zJ = \beta J, \text{ or } itJ/\hbar, \quad (15)$$

where all the dimensionless quantities are shown explicitly. In the complex- y plane, $y = 1$ corresponds to the infinite temperature case and the $t = 0$ state. Henceforth, we set $\hbar = k_B = 1$

III. EARLY-TIME BEHAVIOUR

The normalization conditions ensure that $f(t = 0) = 0$. In the complex- y plane, f is analytic around $y = 1$ which corresponds to $t = \beta = 0$. For small values of t , a Taylor series expansion of $f(t)$ can be performed, and analyticity around $y = 1$ guarantees that the derivatives there are independent of the direction in the complex plane (Cauchy-Riemann conditions). As a result, the thermal free-energy's high-temperature behavior determines the behavior of $f(t)$ at early times.

Expanding the exponentials in Eq. (3b),

$$e^{iE_n t} = 1 + iE_n t - \frac{1}{2} E_n^2 t^2 + \dots,$$

we can write the rate function or the free energy (Eq. (5) per bond as

$$f(t) = \frac{\langle E^2 \rangle - \langle E \rangle^2}{B} t^2 + O(t^3), \quad (16a)$$

where the averaging $\langle \dots \rangle$ is done over the probability distribution at $t = 0$ (see Eq. 3b). There is no linear term in t because f involves only the real part. The quadratic dependence on t is consistent with time reversibility under the unitary evolution of the initial state with H .

The specific heat (per bond) is given by the energy fluctuation

$$c(\beta) = \frac{\langle E^2 \rangle_\beta - \langle E \rangle_\beta^2}{B} \beta^2, \quad (16b)$$

where $\langle \dots \rangle_\beta$ denotes the thermal average at inverse temp β . For $\beta \rightarrow 0$, $c(\beta) \sim \beta^2$ because the energy spectrum for the model is bounded, and the variance is extensive (i.e., $\propto B$). In other words, if the high temperature specific heat

$$c \approx \frac{C_0}{T^2}, \text{ such that } C_0 = \lim_{T \rightarrow \infty} T^2 c(T),$$

the initial t dependence of the rate function during the quantum quench is

$$f(t) \approx C_0 t^2, \text{ (small } t), C_0 > 0. \quad (16c)$$

Eq. (16c) connecting the quench behaviour to the specific heat is a general result valid for any H with bounded spectrum, provided the quench is from a state of uniform distribution of states.

IV. IMPLEMENTING RG IN THE COMPLEX PLANE

The procedure adopted in this paper is the real-space renormalization group. The scale invariance of the hierarchical lattices (Sec. II A) allows us to decimate (integrate out a set of degrees of freedom) exactly and repeatedly. The exact decimation gives us the renormalized parameters for the decimated lattice, as well as the transformation of the rate function.

Below is a summary of the basic steps, which are further illustrated through diagrams in Appendix A. The rate function is also expressed as a sum over the renormalized parameters (here y), with an additional boundary term that is needed in our discussion of the one-dimensional case.

The RG analysis involves a partial summation of a subset of spins to define a new effective parameter for the remaining spins. The protocol would be as follows [37, 38].

1. Let us start with a large lattice and sum over the spins represented by the red squares in Fig. 1.
2. The partial partition functions correspond to the weights (Boltzmann factors for the thermal problem) for the remaining spins. In our case, the b -branched diamond reduces to a single bond connecting the blue spins. (The *decimation step*)
3. The partial partition function of a diamond of b branches with the two blue spins in the same state, say state $\alpha = 1$ is $Z_{\text{dia}}(y|\alpha, \alpha) = (y^2 + 2)^b$ which is proportional to the partition function of a bond with the renormalized weight y' , $Z_{\text{bond}}(y'|1, 1) = y'$. There are q such partition functions, and all are equal.
4. The partial partition function for the blue spins in different states, α and $\beta \neq \alpha$ is $Z_{\text{dia}}(y|\alpha, \beta) = (2y + 1)^b$ which should be proportional to the weight of a renormalized bond connecting two different spins, $Z_{\text{bond}}(y'|\alpha, \beta) = 1$. By symmetry, there are $q(q-1)$ such partition functions, and all are equal.
5. There are two RG equations to determine the renormalized parameter y' and the proportionality factor $c(y)$. The RG equations are

$$(y^2 + 2)^b = cy', \text{ and } (2y + 1)^b = c, \quad (17a)$$

and, therefore,

$$y' = R(y) = \left(\frac{y^2 + 2}{2y + 1} \right)^b, \text{ and } c = (2y + 1)^b \quad (17b)$$

This completes the *rescaling step*.

6. The total partition function, with $q = 3$ is

$$Z(y) = qZ(y|\alpha, \alpha) + q(q-1)Z(y|\alpha, \beta), \quad (18a)$$

which should be invariant under the RG transformation. The invariance requirement is satisfied by the proportionality factor $c(y)$. The partition function for the n th generation $Z_n(y)$ is related to $Z_{n-1}(y')$ by

$$Z_n(y) = Z_{n-1}(y') c(y)^{B_{n-1}}, \quad (18b)$$

with

$$Z_1(y) = q(y + q - 1) \quad (18c)$$

7. The Loschmidt rate function per bond is calculated along the RG trajectory from the repeated application of $R(y)$. We denote the n th iteration by [45]

$$R^{(n)}(y) \equiv R(R(\dots R(y))), \quad (19a)$$

and use

$$y^{(j)} \equiv R^{(j)}(y), \text{ with } y^{(1)} = y', y^{(0)} = y. \quad (19b)$$

The rate function is then given by (in the full complex form)

$$f_n(y) = -\frac{1}{B_n} \ln Z_n(y) \quad (20a)$$

$$= \frac{1}{2b} f_{n-1}(y') + \frac{1}{2b} g(y), \quad (g(y) = \ln c(y)), \quad (20b)$$

$$= \sum_{j=0}^{n-1} \frac{1}{(2b)^j} g(y^{(j)}) + \frac{1}{(2b)^n} \ln Z_1(y^{(n)}). \quad (20c)$$

Eq. (20c) is rapidly convergent and can be used to compute the Loschmidt echo numerically for large n . We obtain $f(y)$ by taking the real part at the end.

The principal branch of the log function is to be used (cut along the negative real axis). However, as the Loschmidt echo is determined by the real part of $f(y)$ (Eq. (20), and the multivaluedness of the log function appears in the imaginary part only, the location of the branch cut is not crucial for the problem at hand.

V. COMPLEX DYNAMICS IN ONE VARIABLE

The gradual thinning of degrees of freedom in the renormalization group approach, as discussed in Sec.

IV, requires repeated applications of the transformation $y' = R(y)$ of the characteristic Boltzmann factor. To address the Loschmidt echo problem, we treat y as a complex variable in the extended complex plane $\hat{\mathcal{C}} = \mathcal{C} \cup \{\infty\}$ which is the Riemann sphere obtained via stereographic projection [46]. Infinity has to be included because the zero temperature corresponds to $\beta, y \rightarrow \infty$.

In contrast to the thermal problem (real y), where fixed points are sufficient, the RG flows in the complex plane require a more detailed understanding of their behavior. These flows can be divided into two categories: the Fatou set and the Julia set. The Fatou set represents the set of points that converge to one of the transformation's attractive fixed points. This set can be considered as the potential phases of the system, but only if the attractive fixed points are accessible from the unit circle ($|y| = 1$). On the other hand, the Julia set is composed of the boundaries of the basins of attractions and includes the repulsive fixed points. It generally contains an infinite number of points and is a dense set.

The study of repeated maps in the complex plane is made possible by the use of complex dynamics methods. This section discusses important aspects such as the classification of fixed points and orbits (Sec. VB), the characteristics of the Julia and the Fatou sets (Sec. VD), providing an overview of the methods and results of complex dynamics.

A. RG as an iterated map

The exact RG transformation, Eq. (17b), is a rational function $R = \mathcal{P}/\mathcal{Q}$, where \mathcal{P} and \mathcal{Q} are polynomials in y . This is because the RG transformation involves partition functions of a small or finite number of degrees of freedom, and is, therefore, nonsingular for real y . In the complex- y plane, there can, however, be poles. The iterated maps of such a function are generally called dynamics in one complex variable, in short, *complex dynamics*. A few general properties of such complex dynamics are summarized here [40–42].

The rational form \mathcal{P}/\mathcal{Q} is such that there are no common factors of \mathcal{P} and \mathcal{Q} . In this situation, if \mathcal{P} and \mathcal{Q} are polynomials of degree p and q ,

$$\mathcal{P}(y) = \sum_{j=0}^p a_j y^j, \text{ and } \mathcal{Q}(y) = \sum_{j=0}^q b_j y^j, (a_p, b_q \neq 0), \quad (21a)$$

the degree of the transformation R is defined as

$$\text{deg}(R) = \max(p, q), \quad (21b)$$

so that there are $\text{deg}(R) + 1$ fixed points (fp) in $\hat{\mathcal{C}}$ as solutions of $R(y) = y$, or $P(y) = yQ(y)$ (counting multiplicities and infinity).

For the thermal problem, with y as a Boltzmann factor, $1 \leq y \leq \infty$, there should be at least two fixed points, (i) $y = 1$ representing the infinite-temperature fixed point

(noninteracting limit), and (ii) $y = \infty$ representing the zero-temperature behaviour (generally an ordered state). In addition, there could be a critical fp representing a transition. Now, for the zero-temperature fixed point, $y' = R(y) \rightarrow \infty$ as $y \rightarrow \infty$, which implies $p > q$. Consequently, the RG transformation should be such that

$$p \geq 2, \quad p > q, \text{ and } \text{deg}(R) = p. \quad (22)$$

B. Fixed points

Let us represent the fps by y_k^* , $k = 1, 2, \dots, \text{deg}(R) + 1$. Each fp y_k^* is characterized by its multiplier (also called eigenvalue)

$$\lambda = \left. \frac{dR(y)}{dy} \right|_{y_k^*}, \quad (23a)$$

which can be used for a classification of the fps as

1. Repelling (unstable) fp, if $|\lambda| > 1$,
2. Attracting (stable) fp, if $0 < |\lambda| < 1$,
3. Super-attracting fp, if $\lambda = 0$, i.e. $R(y) = y_k^* + c_m(y - y_k^*)^m + \dots$, for some integer $m \geq 2$
4. Neutral, if $\lambda = e^{i2\pi\theta}$, $|\lambda| = 1$, with three possibilities,
 - (a) $\theta = 0$, so that $R(y) = y + c_2(y - y_k^*)^2 + \dots$,
 - (b) $\theta = m/n$ so that $\lambda^n = 1$ for integers m, n ,
 - (c) θ is not a rational fraction.

Neutral points do not occur in this paper.

For an fp at ∞ , $R(\infty) = \infty$, the multiplier is determined by the behaviour of $\tilde{y} = 1/y$ with the transformed map $1/R(1/\tilde{y})$. The multiplier is then given by

$$\lambda = \frac{1}{\left. \frac{dR(y)}{dy} \right|_{\infty}}, \quad (23b)$$

which can be used for its classification in the above scheme.

C. Periodic orbits

The RG trajectory or orbit for any point y_0 is the sequence of numbers, $y^{(n)} \equiv R^{(n)}(y_0)$ (see Eq. (19a)),

$$y_0 \xrightarrow{R} y^{(1)} \xrightarrow{R} y^{(2)} \dots \xrightarrow{R} y^{(n)} \dots \quad (23c)$$

If $y^{(n)} = y_0$ for some integer n , then the trajectory is periodic, a cycle of order n for the smallest integer n . The multiplier λ for a cycle is given by

$$\lambda = \left. \frac{dR^{(n)}}{dy} \right|_{y_0} = \prod_{j=0}^{n-1} \left. \frac{dR}{dy} \right|_{y^{(j)}}, \quad (23d)$$

and the product formula follows from the chain rule. Note that λ is independent of the starting point y_0 . The cycles can then be classified by the value of the multiplier at the fixed points of $R^{(n)}(y)$. A periodic orbit (also called a cycle) indicates that the RG transformation simplifies if it is based on a larger cell. However, the small-scale periodicities would show some nice properties at a local level. We shall see such examples in this paper.

D. Julia set and Fatou set

The extended complex plane $\widehat{\mathbb{C}}$ (i.e., the Riemann sphere) can be divided into two broad categories based on how the RG trajectories approach the fps. One set, to be called the Fatou set, consists of points whose RG trajectories approach any attractive fp or periodic cycle. This set includes the basins of attraction (not necessarily connected) of all the attractive fps. The second category, named the Julia set, $J(R)$ of the transformation R , is the boundary of the Fatou set, and $J(R)$ consists of points whose trajectories may behave chaotically. The trajectories remain confined to the set. The importance of the Julia set is discussed below, but before that, we summarize [40–42] some of the properties of the two sets here.

1. Trajectories on $\widehat{\mathbb{C}}$ are considered equicontinuous when two points maintain their proximity throughout their paths [47]. All such equicontinuous trajectories belong to the Fatou set, which, as already mentioned, need not be a connected set. It should be noted, however, that any attractive fixed point possesses a connected neighbourhood, no matter how small, where the multiplier λ can accurately depict the trajectories.
2. If the trajectories behave chaotically, i.e., there is a sensitive dependence on the initial point, and the equicontinuous definition [47] fails, then y_0 , the starting point, belongs to the Julia set. The points of the Julia set transform among themselves under R and do not flow to any attracting fp.
3. The Fatou set is open, and the Julia set is its boundary. The Julia set is dense with dimension $\dim J \leq 2$ as $J \subset \widehat{\mathbb{C}}$
4. All attracting fixed points and cycles belong to the Fatou set.
5. All repelling fps and periodic orbits belong to the Julia set.
6. If y belongs to $J(R)$ then $R(y) \in J(R)$. It follows that $J(R^{(n)}) = J(R)$, for any n . In other words, the Julia set of the n -fold iterate is the same as the Julia set of R .
7. If degree $\deg(R) \geq 2$ (Eq. (22)), then there are no isolated points in $J(R)$.

The Julia set is crucial in determining the phase transitions discussed in this paper. Specifically, the unstable fixed points and periodic points of the RG transformation, located at the intersections of the Julia set with the unit circle or the positive real axis, are of utmost importance. Moreover, the stable fps belonging to the Fatou set determine the phases of the system, provided that an RG trajectory takes an initial point on the unit circle to that fp. Finally, the Julia set is also connected to the zeros of the partition function. This connection makes the intersections of the unit circle $|y| = 1$ with the Julia set at points other than fixed points important as possible candidates for singularities.

VI. ZEROS AND JULIA SETS

The partition function for a finite lattice of B_n bonds is a polynomial in y of degree B_n . The highest power of y comes from the threefold degenerate ground state, and this term is $3y^{B_n}$. There are B_n zeros of Z_n in the complex- y plane. We establish the connection between the zeros of the partition function and the Julia set through the renormalization group transformation [38].

The partition function for the n th generation, with B_n bonds, is connected to that of the $(n-1)$ th generation by the RG transformation as given by Eq. (18b). By denoting the zeros of Z_n by ζ_j and those of Z_{n-1} by ζ'_k , we rewrite Eq. (18b) as

$$\prod_{j=1}^{B_n} (y - \zeta_j) = \left[\prod_{k=1}^{B_{n-1}} (y' - \zeta'_k) \right] c(y)^{B_{n-1}}, \quad (24a)$$

$$= \prod_{k=1}^{B_{n-1}} [(y^2 + 2)^b - (2y + 1)^b \zeta'_k], \quad (24b)$$

where the second line follows from the substitution of $c(y)$ and y' from Eqs. (17b). Each factor of the right-hand side of Eq. (24b) is a polynomial of degree $2b$, which means that for a given zero ζ'_k of Z_{n-1} , there are $2b$ roots of the polynomial, which, in turn, represent the zeros of Z_n . As a result, ζ_j , the solutions of $Z_n(y) = 0$ are the roots of $R(y) = \zeta'_k$ for every ζ'_k , the solutions of $Z_{n-1}(y) = 0$. In short, ζ_j are the preimages of ζ'_k .

By starting with the zeros of the smallest lattice, successive preimages can be constructed. In the limit of a large lattice (= a large number of iterations), the preimages inevitably converge on the Julia set of the map. This convergence on the Julia set is because the preimages cannot be attractive fixed points. The exceptional cases are those where the initial zero is a fixed point of the RG transformation. Such exceptional cases appear in the one-dimensional case discussed below.

VII. ONE DIMENSIONAL POTTS MODEL ($b = 1$)

We now implement the RG procedure for the one-dimensional problem, which corresponds to the $b = 1$ case as shown in Fig. 1. Two cases are to be distinguished, (i) an open chain, constructed as in Fig. 1, and (ii) a periodic chain (pbc: periodic boundary condition).

In the following text, we discuss the RG transformation and its fp behavior. We then use this transformation to examine chains with open boundary conditions (Sec. VII A) and periodic boundary conditions (Sec. VII B). Although the RG flow remains the same, the DQPT behavior differs, and we explain this aspect in Sec. VII A 1. In Sec. VII D, we elaborate on the differences between the thermal case and the quantum case, especially the role of boundary conditions. Furthermore, we explore the nature of DQPT in Sec. VII C. In Sec. VII E, we utilize a transfer matrix approach [30] to support and augment the results from complex dynamics.

The RG transformation $y' = R(y)$ is given by a rational function (see Eq. (17b) and $b = 1$)

$$R(y) = \frac{y^2 + 2}{2y + 1}, \quad (25)$$

which is of degree $\deg(R) = 2$ (see Eq. (21b)). There are, therefore, only three fixed points, which are given below with their multipliers (λ), as

$$y^* = \begin{cases} 1, & (\lambda = 0), \text{ the high temperature fp} \\ \infty, & (\lambda = 2), \text{ the zero temperature fp} \\ -2, & (\lambda = 0), \text{ unphysical fp} \end{cases} \quad (26)$$

See Fig. 2.

For the thermal behaviour, $y^* = 1$ is the high temperature fixed point that corresponds to the disordered state, while $y^* = \infty$ corresponds to the zero temperature three-fold degenerate ordered state. The third f.p., though it plays no role in the thermal behaviour, is important for the quantum problem. Incidentally, the magnitude of this fp ($|y^*| = 2$) represents the multiplicity of the spin states that do not contribute to the energy [48].

In the RG framework, the stable fixed points ($\lambda < 1$) represent the phases of the system, while the unstable points are the points of phase transitions (thermodynamic critical points). The stabilities are determined by the multipliers of the fps. The zero temperature ordered state is unstable ($\lambda > 1$) in one dimension, consistent with the Landau argument [30] for any system with discrete symmetry. The flow along the real axis to the attracting fp at $y^* = 1$ indicates the lack of any phase transition, or, equivalently, the lack of any ordered state at any non-zero temperature.

In the complex- y plane, $R(y)$ has a pole at $y_0 = -\frac{1}{2}$, such that $R(y_0) = \infty$. Moreover, for any $y_\eta = -\frac{1}{2} + i\eta$, (real η)

$$R(y_\eta) = -\frac{1}{2} + i\eta', \text{ where } \eta' = R_p(\eta) = -\frac{9}{8\eta} + \frac{\eta}{2}. \quad (27)$$

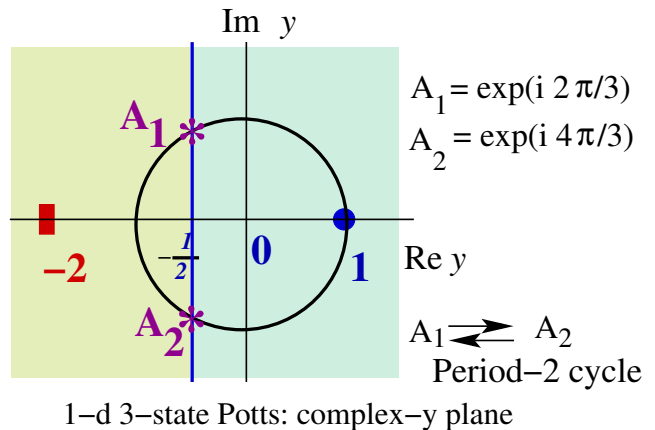


FIG. 2. RG behaviour in the complex- y plane for the Potts chain. Quantum time evolution takes place along the unit circle ($|y| = 1$ or $y = e^{i\theta}$), while the thermal behaviour comes from the positive real axis, notably $1 < y < \infty$. The blue vertical line at $\text{Re } y = -1/2$ is the Julia set for the RG transformation $R(y)$ which has three fps, two attractive fps at $y^* = 1$, $y^* = -2$, and a repulsive fp at $y^* = \infty$. A_j , ($j = 1, 2$) represent a *periodic cycle of period 2*. The points on the arc from A_1 to A_2 on the right side (darker region) flow to $y^* = 1$, while those on the arc on the left side (lighter region) of the blue line flow to $y^* = -2$.

As the RG trajectory of any point on this line stays on the line, the map can also be described by R_p for real arguments. One notes that the two imaginary fixed points ($\eta^* = \pm i3/2$) of $R_p(\eta)$ are just the two finite fps ($y^* = -\frac{1}{2} + i\eta^* = 1, -2$) of Eq. (26).

A. Open boundary condition

For the open boundary condition, the partition function for a single bond, Eq. (18c) has a zero at $y = -2$, which also happens to be a fp. Therefore, the partition function for the open chain, as discussed in Sec. VI, has a multiple zero at the isolated point $y = -2$. The Loschmidt amplitude for B bonds, by Eq. (24), is given by

$$L(t) = \frac{1}{3^B} (y + 2)^B, \quad (28a)$$

with the rate function, Eq.(20), for $y = e^{iJt}$ given by

$$f(t) = -\text{Re} \ln \frac{y + 2}{3} = -\frac{1}{2} \ln \frac{5 + 4 \cos Jt}{9}. \quad (28b)$$

See Fig. 3 for a plot of $f(t)$. There is no DQPT in an open chain, as was shown in Ref [2]. The duality transformation of the one-dimensional classical chain where each bond acts as a Potts spin in a field with no interaction, leads to an innocuous oscillation characterized by one isolated zero of the partition function.

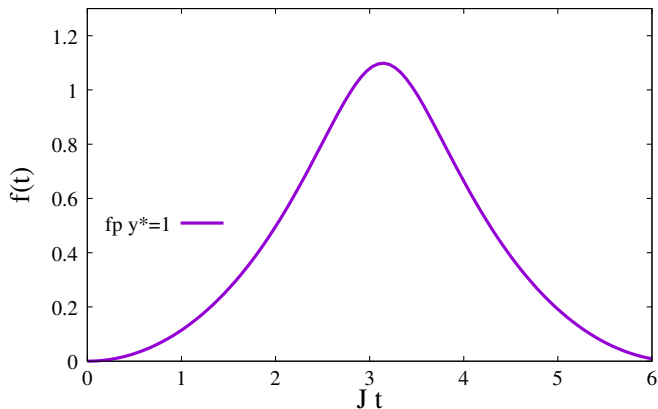


FIG. 3. Loschmidt rate function $f(t)$ vs. t for the Potts chain under open boundary condition. There is no DQPT but oscillations with periodicity $Jt = 2\pi$. This function is the characteristic of the phase that corresponds to the fixed point $y^* = 1$.

1. Contradiction with RG?

The absence of any singularity in $f(t)$ apparently contradicts the results of RG, which, from the flow to the fixed points, predict phase transitions at A_1 and A_2 . The clue is in the boundary term in Eq. (20c), which is determined by the partition function of the smallest structure at the renormalized y . We show that the boundary term itself is singular, and there is a perfect cancellation of the singularity from the sum on the rhs of Eq. (20c). More detailed discussion is given in Sec. VIII E 1.

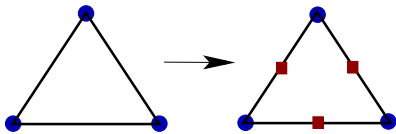


FIG. 4. A periodic chain constructed hierarchically. Each bond of the triangle (generation $n = 0$) goes through the iteration process of Fig. 1a. The number of bonds for generation n is $B_n = 3 \times 2^n$.

B. Periodic boundary condition

For the periodic boundary condition, the construction starts with the triangle, Fig. 4, whose partition function is given by

$$Z_{\Delta} = 3y^3 + 18y + 6, \quad (29)$$

with a total of 27 states (i.e., $Z_{\Delta} = 27$ for $y = 1$). The preimages of the three zeros,

$$-0.32748000207\dots, 0.16374000103\dots \pm i2.4658532729\dots, \quad (30)$$

on successive back iterations, approach either infinity or a point on the line $z = -1/2 + i\eta$ (Eq. (27)), which is the Julia set for $R(y)$. As the point at infinity (a single point on the Riemann sphere) is unstable (repulsive), it belongs to the Julia set as well.

The points on the complex plane are separated into two groups by the Julia set. These groups belong to either the basin of attraction for the attracting fixed point $y^* = 1$, or the basin for the attracting point $y^* = -2$. Incidentally, these are the only two critical points of the map.

The Julia set intersects the unit circle at two points, namely $A_1 = e^{i2\pi/3}$, $A_2 = e^{i4\pi/3}$ (Fig. 2). These two points form a *periodic cycle of order two*. There is a uniform density of zeros along the vertical line at the intersection point. Such a uniform density is a signature of a first-order transition which is indicated by a slope discontinuity of the rate function.

We now combine the results to see the behaviour of the Loschmidt echo. At time $t = 0$, the rate function $f(t) = 0$. As time progresses, the system moves towards A_1 along the unit circle in the anticlockwise direction, Fig. 2, but the rate function is just an analytic continuation of the initial state described by the attracting fp $y^* = 1$ (high temperature, disordered state). Except for the time interval from A_1 to A_2 , i.e. between

$$t_{c1} = \frac{2\pi}{3} \frac{1}{J}, \text{ and } t_{c2} = \frac{4\pi}{3} \frac{1}{J}, \quad (31)$$

the Potts chain behaves as a disordered phase characterized by the high temperature fp $y^* = 1$ with $f(t)$ given by Eq. (28b). There is no difference between the open and periodic boundary conditions because the spins (or, rather, dual spins) behave independently. For the time

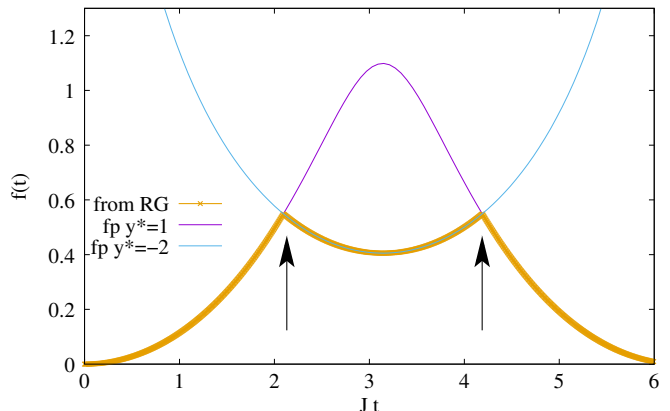


FIG. 5. The rate function vs time (Jt) for the periodic Potts chain. The results from the sum of 60 terms (Eq. (20c)) is shown by the thick line which shows two points (indicated by arrows) with slope discontinuities at $Jt_{c1} = 2\pi/3$, and $Jt_{c2} = 4\pi/3$. There is a periodicity—the transitions are seen at $Jt_{c1} + 2\pi n$, $Jt_{c2} + 2\pi n$ for any integer n . The rate functions characteristic of the two fps ($y^* = 1, -2$) are denoted by the thin lines (Eqs.(28b) and (39d)). These overlap within numerical accuracy with the data points.

interval between A_1 , A_2 , given by Eq. (31), the rate function is characteristic of the fp $y^* = -2$. (Eq. (39d)). There is a periodicity, and the transitions take place at $t_{c1} + 2\pi n/J$, and $t_{c2} + 2\pi n/J$, for integer n . These transitions were pointed out in Ref. [10]. There is a phase that has no analog in the thermodynamic system.

C. The Nature of transitions

To explore the nature of the phase transitions, we first note that A_1 and A_2 form a period-2 cycle so that each one is a repulsive fixed point of $R^{(2)}$ with multiplier $\lambda = 2^2$, (see Table II of Appendix C). The RG transformation $R^{(2)}$ requires a decimation of exactly four bonds, which results in a length rescaling factor of $s = 4$. Therefore, in this one-dimensional ($d = 1$) case, $\lambda = s^d$. This relationship between the fixed point's λ and the rescaling factor s is a characteristic of a “discontinuous” fixed point for a first-order transition [49].

We now show that $f(y)$ has slope discontinuities at the transition points. Let us assume power-law singularities around such a “discontinuous” fp, generically denoted by y_c , of the form

$$f(y) \sim f_0 |y - y_c|^{2-\alpha}, \quad (32a)$$

using the standard notation for critical exponents [30, 32].

The relation for the free energy as given by Eq. (20b) can be written in terms of $R^{(2)}$ as

$$f_n(y) = \frac{1}{2^2} f_{n-2}(R^{(2)}(y)) + g_2(y), \quad (32b)$$

where $g_2(y) = \frac{1}{2} \ln c(y) + \frac{1}{2^2} \ln c(R(y))$ is an analytic function around each of the fps ($y = R^{(2)}(y)$)

$$y_{c1} = e^{i2\pi/3} \text{ and } y_{c2} = e^{i4\pi/3}.$$

Expanding around y_c ,

$$R^{(2)}(y) = \lambda (y - y_c), \text{ with } \lambda = 2^2, \quad (32c)$$

we rewrite Eq. (32b) for large n (when $f_n(y)$ is independent of n) as

$$f(y) \approx \frac{1}{2^2} f(R^{(2)}(y)), \quad (32d)$$

which implies, for the singular part,

$$|y - y_c|^{2-\alpha} = \frac{\lambda^{2-\alpha}}{2^2} |y - y_c|^{2-\alpha}, \quad (32e)$$

so that

$$\frac{\lambda^{2-\alpha}}{2^2} = 1, \text{ or, } \alpha = 1, \quad (32f)$$

i.e., $f(y)$ behaves linearly near y_c . Therefore, at both the points A_1, A_2 , there are slope discontinuities in $f(t)$ as seen in Fig. 5. The transitions in time are akin to first-order transitions. Surprisingly, the transitions are described by a cycle of period-2 or by fps of bigger blocks for RG, rather unusual when compared with thermal phase transitions.

D. Open versus periodic boundary conditions

The rate function $f(t)$ for the Potts chain depends on the boundary condition (bc) imposed on the chain, open or periodic (see Sec. VII A-C). This difference contradicts the typical behavior observed in thermodynamic systems' bulk behavior. The open chain, with free boundary spins, does not exhibit DQPT, while the periodic chain does, despite having identical RG flow equations and fixed points.

The distinction arises from the remainder or boundary term, (see Sec. VII A 1)

$$b_n = 2^{-n} \ln Z_1(y^{(n)}), \quad (33)$$

in the RG computation of the rate function, Eq. (20c). The behaviour of b_n for $n \rightarrow \infty$ is analyzed below for the thermal and the quantum cases.

1. Thermal case

The boundary term, Eq. (33), in the $n \rightarrow \infty$ limit requires the fp value of y . For the thermal problem (real y), the partition function for the finite system is never zero and, therefore, $2^{-n} \ln Z_1 \rightarrow 0$. In this case, the free energy is determined solely by the sum of the contributions from the RG factors $g(y^{(j)})$ (Eq. (20c)), and *the summation is independent of the boundary conditions.*

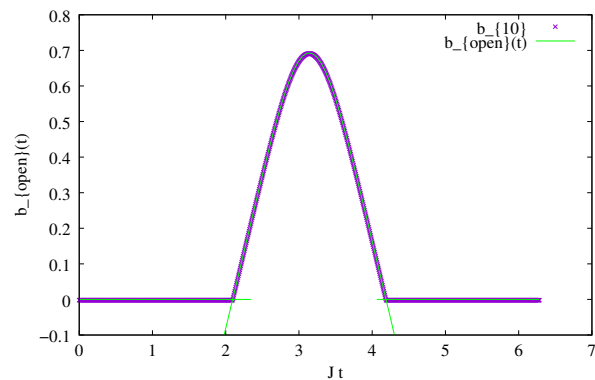


FIG. 6. The remainder term $b_{open}(t)$ -vs- Jt for the open 3-state Potts chain. Eqs. (34c),(34d) for the rate function (green solid line for $2\pi/3 < Jt < 4\pi/3$) compares well with the numerically evaluated values of b_n for $n = 10$. The green lines have been extended beyond the intersections for clarity.

2. Quantum case

We now consider Eq. (33) for the quantum case. For large n , $y^{(n)}$ approaches one of the two attractive fixed points, $y^* = 1$, or -2 (for the Potts chain), both of which belong to the Fatou set.

We can categorize the possibilities into two groups. Typically, the Julia set is comprised of the zeros of the

partition function, while the Fatou set represents the different phases of the system. Nevertheless, there is the second scenario when the zeros are the attractive fixed points within the Fatou set. These two cases form the basis of the boundary-condition dependent dichotomy. The results (proved below) can be stated as a mathematical mechanism as follows.

Theorem (Boundary). *If an attractive fixed point of the RG transformation, which is a member of the Fatou set, coincides with the zero of the partition function, the boundary contributions become as significant as the bulk rate function. If the singularities cancel out exactly, the phase linked to that fixed point would not appear.*

We establish this theorem under various boundary conditions.

a. Periodic chain: For the periodic case, the remainder term is determined by $Z_{\Delta}(y^{(n)})$ (the first generation lattice), which approaches a finite non-zero number so that $b_n \rightarrow 0$ as $y \rightarrow y^*$. This is the generally expected result, and the RG flow determines the nature of $f(t)$. *A DQPT ensues.*

b. Open chain For the open boundary case, we note that Z_1 approaches a constant when $y^{(n)} \rightarrow 1$, and the remainder term vanishes ($b_n \rightarrow 0$) in the limit. In contrast, over the region characterized by $y^{(n)} \rightarrow y^* = -2$, extra care is needed because $Z_1 = 3(y^{(n)} + 2) \rightarrow 0$.

Defining $z_n = 3(y^{(n)} + 2)$, the recursion relations for z_n and b_n can be written with the help of the RG equation $y' = R(y)$ as

$$z_{n+1} = 3(R(y) + 2) = \frac{z_n^2}{2z_n - 9}, \quad (34a)$$

$$b_{n+1} = b_n - \frac{1}{2^{n+1}} \ln(2z_n - 9). \quad (34b)$$

These relations allow us to evaluate the boundary-dependent remainder term, $b_{\text{open}}(y)$ as

$$b_{\text{open}}(y) \equiv \lim_{n \rightarrow \infty} b_n = \begin{cases} 0, & \text{for } y^* = 1, \\ \text{nonzero}, & \text{for } y^* = -2. \end{cases} \quad (34c)$$

It follows that $b_{\text{open}}(y)$ is singular at A_1, A_2 , the transition points of Fig. 5.

Numerically evaluated $b_{\text{open}}(t)$ is shown in Fig. 6 and is compared with the following ansatz,

$$b_{\text{open}}(t) = \frac{1}{2} \ln \frac{2 - 2 \cos(Jt)}{5 + 4 \cos(Jt)}, \quad \frac{2\pi}{3} < Jt < \frac{4\pi}{3}. \quad (34d)$$

The exact cancellation of the singularities of $f(t)$ of the periodic chain (the bulk contribution) by the boundary terms gives us the analytic behaviour of the open chain of Fig. 3. There is no DQPT in this case.

The above arguments predict that there will be no DQPT if one boundary spin is kept fixed while the other end is free. Instead, if both the boundary spins are held fixed, there will be DQPT. A few cases are listed in Table I. These predictions are verified in the next section by the transfer matrix approach [10].





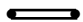
Boundary Conditions	Chain type ($n = 1$)	Partition function $Z_1(y)$	DQPT?
Open	 free free	$3y + 6$	No
Open	 fixed free	$y + 2$	No
Open	 fixed fixed	y (if parallel) 1 (nonparallel)	Yes
Periodic		$3y^3 + 18y + 6$	Yes
Periodic		$3y^2 + 6$	Yes

TABLE I. Boundary conditions and DQPT. An arrow indicates a spin of fixed orientation, while a bullet or a light vertex indicates a spin that takes all 3 possible orientations. The end point conditions are preserved as the lattice is built hierarchically.

E. Intermediate phase and Transfer matrix

The rate functions are evaluated so far with the help of the series of Eq. (20c). To analyze the intermediate behaviour, we utilize the transfer matrix approach[30]. The partition function for a chain of B bonds can be expressed as a 3×3 matrix which can be constructed by repeated multiplication of 3×3 symmetric transfer matrices

$$\mathbb{M} = \begin{pmatrix} y & 1 & 1 \\ 1 & y & 1 \\ 1 & 1 & y \end{pmatrix}, \quad (35)$$

so that after B steps, the partition function with the first spin in state α_j and the last spin in state α_k ($j, k = 1, 2, 3$) is given by

$$Z(y|\alpha_j\alpha_k) = \mathbb{M}^B|_{jk}. \quad (36)$$

For the periodic boundary conditions, we identify the first and the last spins, and therefore, the total partition function is

$$Z_{\text{pbc}}(y) = \text{Tr } \mathbb{M}^B. \quad (37)$$

For the open boundary conditions, the first and the last spins are independent, and the partition function involves a sum over all the 9 possible combinations, i.e., the sum of all the terms of the Z matrix so that

$$Z_{\text{open}}(y) = \text{Tr } \mathbb{M}^B + 6Z(y|\alpha_j\alpha_k), (j \neq k). \quad (38)$$

These extra off-diagonal terms do not contribute to the thermodynamic behaviour but are vital for the quantum problem.

The eigenvalues of \mathbb{M} are [50]

$$\Lambda_1 = y + 2, \quad \Lambda_2 = y - 1 \quad (39a)$$

where Λ_2 is doubly degenerate. Thanks to the symmetric form of \mathbb{M} , the eigenvector of Λ_1 is $(1, 1, 1)/\sqrt{3}$, while the other two can be chosen as $(-1, 0, 1)/\sqrt{2}$, $(-1, 2, -1)/\sqrt{6}$. The eigenvectors are all real, orthogonal, and independent of y , allowing us to write [51]

$$\mathbb{M}^B = \frac{1}{3^B} \begin{pmatrix} a & b & b \\ b & a & b \\ b & b & a \end{pmatrix}, \quad \text{with} \quad \begin{cases} a = \Lambda_1^B + 2\Lambda_2^B, \\ b = \Lambda_1^B - \Lambda_2^B \end{cases} \quad (39b)$$

so that

$$\begin{aligned} Z_{pbc}(y) &= \frac{1}{3^B} (\Lambda_1^B + 2\Lambda_2^B) \\ &=_{B \rightarrow \infty} \begin{cases} (\Lambda_1/3)^B & \text{if } |\Lambda_1| > |\Lambda_2| \\ (\Lambda_2/3)^B & \text{if } |\Lambda_1| < |\Lambda_2| \end{cases} \end{aligned} \quad (39c)$$

For real y , $1 \leq y < \infty$, we have $\Lambda_1 \geq \Lambda_2$, equality only for $y \rightarrow \infty$, and the free energy of the Potts chain per bond is given by $-k_B T \ln \Lambda_1$ for all temperatures. However, for the quantum problem with $y = \exp(iJt)$, there is a crossing of the eigenvalues with degeneracy occurring on the unit circle $|y| = 1$. When $|\Lambda_2| > |\Lambda_1|$, the rate function per bond is given by

$$f(t) = -\text{Re} \ln(\Lambda_2/3) = -\frac{1}{2} \ln[(2 - 2 \cos Jt)/9], \quad (39d)$$

as shown in Fig. 5. This form is observed for $t_{c1} \leq t \leq t_{c2}$, the range in which y flows to the fp $y^* = -2$. There is no analog of this phase in the one-dimensional magnet.

Since the phase transition occurs at the point of degeneracy of the distinct eigenvalues, a diverging length scale appears close to the transition point as

$$\xi = \left| \ln \left| \frac{\Lambda_1}{\Lambda_2} \right| \right|^{-1}, \quad (39e)$$

such that $\xi \rightarrow \infty$ as $t \rightarrow t_{c1} \pm$ or $t \rightarrow t_{c2} \pm$. This diverging length scale is to be interpreted as a finite-size length scale such that for a finite system, deviations from the sharp transition is seen for $B < \xi(t)$.

By using the known eigenvalues Eq.(39a), the divergence of ξ is given by

$$\xi \sim |t - t_c|^{-1}, \quad \text{both for } t_c = t_{c1} \text{ and } t_{c2}, \quad (39f)$$

and to see the sharpness of the transition, we need to respect $B \gg \xi$. Or, finite B data can be made to collapse on a master curve (data collapse) [52] if B/ξ is used as a scaling behaviour. Therefore, for a chain of B bonds, the rate function $f_B(t)$ per bond satisfies a scaling form

$$f_B(t) \equiv f(t_c) + B \mathcal{F} \left(\frac{B}{\xi(t)} \right), \quad (39g)$$

where the scaling function

$$\mathcal{F}(x) \approx f_{\pm} \frac{1}{x}, \quad \text{as } t \rightarrow t_c \pm. \quad (39h)$$

with f_{\pm} determining the jump in the slope at t_c . It is straightforward to verify such a data collapse from numerics.

The same scale ξ determines the spatial exponential decay of spin-spin correlations in both the phases characterized by $y^* = 1$ and $y^* = -2$, indicating that these phases are paramagnetic.

1. Importance of freedom

The RG analysis can be compared with the transfer matrix results. In the open chain case, Eq. (38) shows a perfect cancellation of the contributions from Λ_2 . However, changes in the free conditions of the boundary spins would tilt the behaviour towards the DQPT case. There is no DQPT if we keep one boundary spin fixed at, say, state-1, so that the partition function involves a summation of the elements across one row of the matrix in Eq. (39b). On the other hand, if the two boundary spins are kept fixed, only one element of the matrix is needed, and *there is DQPT*. All the entries of Table I can be verified with the help of Eq. (39b).

VIII. HIGHER DIMENSIONS ($d > 1$)

Dimensionality (d) is important in determining the nature of phase transitions in classical and quantum systems. We expect d to be important for DQPT, too, thanks to the intimate connection between DQPT and classical phase transitions. For example, in classical systems with finite range interactions and discrete symmetry, a transition occurs for $d > 1$ (Peierls' argument) but not in $d = 1$ (Landau's argument) [30]. From the perspective of the renormalization group, these results mean that the zero-temperature fixed point ($y^* = \infty$), which is unstable for $d = 1$ (see Eq. (26)), must become stable for $d > 1$. An immediate consequence is that the Julia set, relevant for DQPT, is compact, i.e., restricted to the finite complex plane.

The following discussion delves into the RG transformation and its fps. We also explore the nature of the Julia set, a fractal, in Sec. VIII A. Furthermore, we examine the DQPTs corresponding to the Julia set's repulsive fps on the unit circle. These fps are analogous to the discontinuous fp for first-order transitions. The details of the transition behaviour can be found in Sec. VIII B, where the rate function $f(t)$ is also obtained.

Let us consider a two-dimensional hierarchical lattice, i.e., with $b=2$ (Sec.II A). The renormalization transformation is now

$$R_2(y) = R(y)^2 = \left(\frac{y^2 + 2}{2y + 1} \right)^2, \quad (40)$$

which is different from $R^{(2)}$ of Eq.(32c).

The complex dynamics protocol reveals that $R_2(y)$ has a degree of four, leading to five fixed points, including the

point at infinity. At low temperatures, the ordered state remains stable, making $y = \infty$ a stable fp with a basin of attraction near the point at infinity in the extended complex- y plane. This region belongs to the Fatou set.

The fixed points and their multipliers are

$$y^* = 1, \quad \lambda = 0, \quad (41a)$$

$$y^* = 4, \quad \lambda = 16/9, \quad (41b)$$

$$y^* = e^{\pm i2\pi/3}, \quad \lambda = 4e^{\mp i2\pi/3}, \quad |\lambda| = 4, \quad (41c)$$

$$y^* = \infty, \quad \lambda = 0. \quad (41d)$$

Of these $y^* = 1$, and ∞ are the two stable (super-attractive, because the multipliers = 0) fixed points representing the para or high-temperature phase and the ordered phase, respectively, with $y^* = 4$ as the thermodynamic critical point (“Curie point”) separating the two phases. The remaining two fixed points are on the unit circle and are repulsive or unstable. These are relevant for DQPT.

A. Nature of the Julia set

A notable difference between $b = 2$ and the one-dimensional $b = 1$ case is the behaviour of the $y = \infty$ fp, which is now a super-attractive fp, with its own basin of attraction. The Julia set, as pointed out earlier, contains an infinite number of points that do not flow to the stable fps [53], (see also Sec. VD).

The RG map has critical points (where the first derivative is either zero or infinity) at

- $y = 1, \infty$ (fp)
- $y = -2, \pm i\sqrt{2}$, (not fps)
- $y = -1/2$ (a pole).

Of these $y = -2, \pm i\sqrt{2}$ are in the Julia set, as repeated iterations give [54]

$$-2 \xrightarrow{R_2} 4 \xrightarrow{R_2} 4, \quad \text{and} \quad \pm i\sqrt{2} \xrightarrow{R_2} 0 \xrightarrow{R_2} 4. \quad (42)$$

The Julia set for R_2 is shown in Fig. 7. The colour code indicates the number of iterations (< 20) required to reach the stable fps ($y^* = 1$ or ∞). The unstable fp at $y^* = 4$ where the zeros pinch the real axis is the classical critical point of the $q = 3$ -Potts model for $b = 2$. The two complex fps are A_1, A_2 of the $b=1$ case, Fig. 2. A closer view of the area around A_1 is shown in Figure 7(b), while Figure 7(c) provides a display of the region close to the imaginary axis on the first quadrant. (See Appendix D for the Julia set only.)

B. Transition points

The intersection points of the Julia set with the unit circle (red circle in Fig. 7) are the transition points for

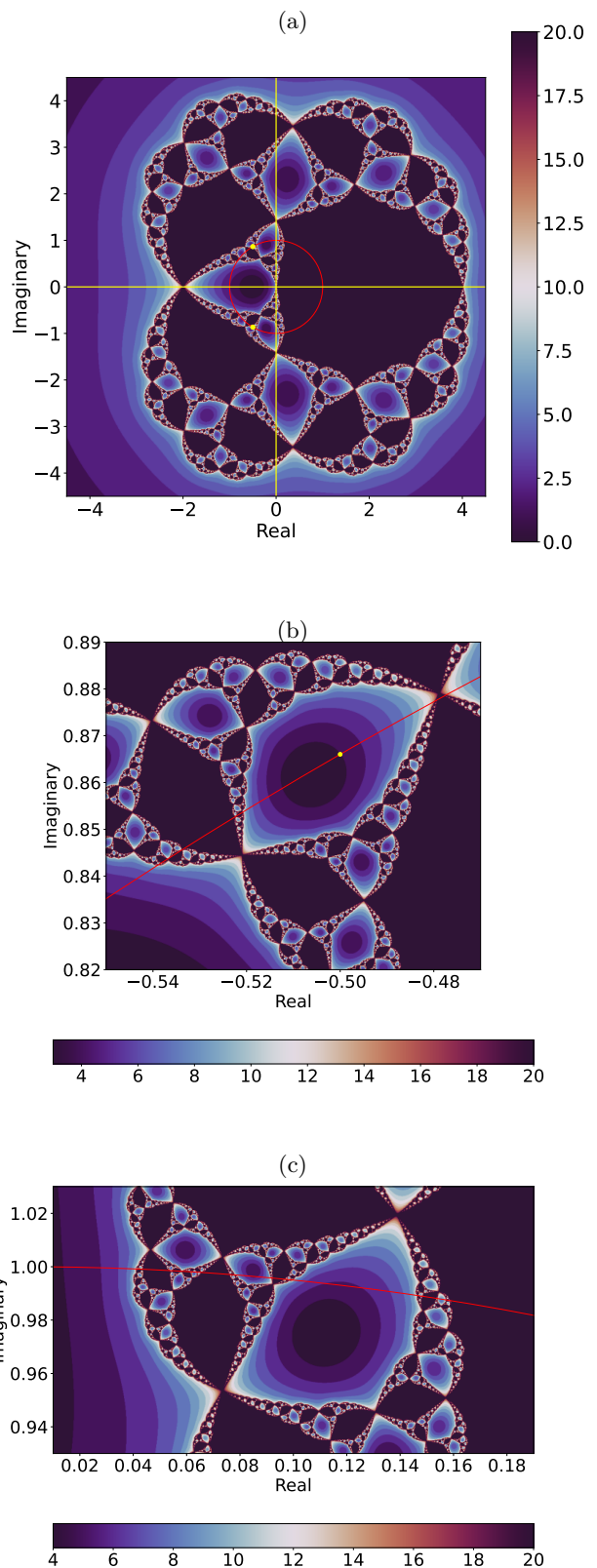


FIG. 7. The Julia set for the $b = 2$ RG transformation R_2 . The colour code represents the number of iterations required (< 20) to reach the stable fps $y^* = 1$ or $y^* = \infty$. The complex fps on the unit circle are represented by yellow dots. The full Julia set is shown in (a) while a magnified image around the fp $y = \exp(i2\pi/3)$ is shown in (b). The intersection of the unit circle with the Julia set in the first quadrant is shown in (c).

DQPT, while the intersection with the positive real axis gives the thermal critical point. The absence of isolated points in the Julia set ensures that the zeros of the partition function for $b = 2$ are not isolated and, therefore, stand for points of phase transitions. Suppose a continuum limit is taken to describe the zeros by a line or surface density of “charges”. In that case, the nature of the transition is completely determined by the behaviour of the density at the intersection point. On the other hand, if the intersection point is an unstable fp, the RG procedure would suffice to determine the transition behaviour.

The unstable fp at $y^* = 4$ describes the thermal criticality of the Potts model. The temperature derivative of the specific heat is divergent (see Eq. (32f)) with

$$\alpha = 2 - \frac{\ln 4}{\ln \lambda} = 2 - \frac{\ln 4}{\ln(16/9)} = -0.4094\dots, \quad (43)$$

where α is one of the critical exponents to describe the symmetry breaking of this particular two-dimensional Potts model.

The two additional fixed points on the unit circle,

$$y^* = e^{i2\pi/3}, \text{ and } e^{i4\pi/3} = e^{-i2\pi/3}, \quad (44)$$

correspond to A_1 and A_2 in Fig. 2.

In the decimation process of the two-dimensional ($d = 2$) lattice, the length is rescaled by a factor of $s = 2$, so that the multiplier can be written as $\lambda = 4 = s^d$. This enables us to identify the two fixed points A_1 and A_2 as “discontinuous” fixed points, which signify first-order transitions.

The RG flow takes y to $y^* = 1$ for the arc A_1 to A_2 on the right side, similar to the $d = 1$ case. However, on the left part of the arc, the flow is to $y = \infty$, indicating that the system is in the ordered state. There is a *symmetry-breaking transition* in time at $Jt_{c1} = 2\pi/3$ and then a *symmetry-restoring transition* at $Jt_{c2} = 4\pi/3$ (periodic para to ferro to para transitions). All these transitions are described by fixed points different from the thermodynamic one.

We determine the exponent α at A_1 (and, by symmetry, identical behaviour at A_2 , though time-reversed) from Eq. (32e) with a rescaling factor of $2b = 4$

$$\alpha = 2 - \frac{\ln 2b}{\ln |\lambda|} = 1, \quad (45)$$

by using the multiplier noted in Eq. (41). This signals a first-order transition (slope-discontinuity of $f(t)$).

A gross feature of the quantum quench in the Potts model is the oscillatory behaviour of para and ferro states with the symmetry-breaking (and restoring) transitions taking place at times t_{c1}, t_{c2} given by Eq. (31). Fig. 8 shows the Loschmidt rate function obtained by using the sum formula of Eq. (20c). The remainder term does not contribute here. The major transition is (Point A_1) described by a fp (Eq. (45)) and is indicated by the

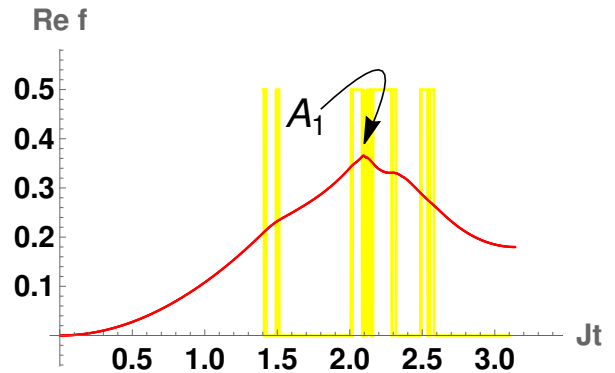


FIG. 8. The rate function $f(t)$ vs t (red solid curve) for $b = 2$. The arrow marks the peak, which represents the location of the first-order transition at $Jt = 2\pi/3 = 2.094\dots$. The yellow vertical lines indicate some of the zeros derived from the intersection of the unit circle $|y| = 1$ with the Julia set. These singularities, which form a dense set, are not described by the listed fixed points but belong to higher-order periodic orbits.

arrow to the peak. The transitions occur periodically at $t_{c1} + 2\pi n/J$ and $t_{c2} + 2\pi n/J$.

In addition to the above gross features, the fractal nature of the Julia set creates finer structures in the time evolution. These structures can be determined by monitoring the flow of y along the unit circle or by studying the unit circle’s intersection with the Julia set. Fig. 7 shows that the unit circle passes through regions of the Julia set, fragmenting the arc of the unit circle into segments flowing to either $y = 1$ or $y = \infty$. Multiple para-ferro-para transitions are expected in a cycle, especially in regions close to $Jt = \pi/2$ and around A_1 . Similar regions also exist in the lower half of the unit circle due to symmetry. Fig. 8 displays the transition points from the flow of y (represented by yellow lines). Unlike the major transitions, these minor transitions are not connected to the fps but, as members of the Julia set, should be related to some higher-order periodic or chaotic orbit. Further exploration of these minor transitions is imperative.

Successive iterations of the RG transformation are equivalent to choosing more spins for decimation. $R_b(y)$ (R or $R_2(y)$ for $b = 1, 2$) is obtained by decimating the motifs one at a time, while $R_b^{(n)}$ would be an RG scheme of a larger step. Therefore, periodic orbits are equivalent to fps of $R_b^{(n)}$ of periodicity n , though it indicates a subtle connection between space and time transformations, respecting time reversibility. Note that in these one-parameter systems, the thermal problem cannot display any periodicity, which is only feasible in the complex plane for the quantum problem.

Both fps, A_1 and A_2 , can be considered as the fps of $R^{(2)}$ in the one-dimensional scenario. Nevertheless, when seen as an iteration of $R(y)$, $A_1 \leftrightarrow A_2$. Decimation in space leads to a transformation of time, causing A_1 to become A_2 . This transformation can be interpreted

as the system being in the future or the past ($e^{iJt} = e^{i(Jt \pm 2\pi)}$), a consequence of the time reversibility of the process.

IX. CONCLUSION

In this paper, we investigated dynamical quantum phase transitions (DQPT) in the quantum 3-state Potts model (Eq. (6a)) using the iterated map formulation (complex dynamics) for exact renormalization group (RG) transformation. We focussed on one and two-dimensional lattices built hierarchically as examples of the exact formulation. The DQPT occurs during the time evolution of the interacting system, and here, we started from a state of uniform superposition of all states that a large transverse field can produce. The time evolution here is unitary and the time scale (restoring \hbar) is tJ/\hbar . This means that there is no classical limit as $\hbar \rightarrow 0$, and the reported phenomena are inherently quantum in nature.

The RG transformation of the Boltzmann factor y is a rational function that divides the complex- y plane into (a) the Fatou set of points that flow to the attractive fixed points (possible phases of the system), and (b) the Julia set consisting of the repulsive fixed points (possible transition points) and repulsive periodic orbits. The Julia set is the boundary of the Fatou set and plays a vital role in the formulation because of its connection to the zeros of the partition function. The description of DQPT requires an analysis of the Julia set, and the RG flows. The rate function determining the Loschmidt echo and the thermodynamic free energy are determined exactly (or numerically exactly) from the RG flows.

From the studies of the open and periodic Potts chains (and other cases), we conclude that the coincidence of an attractive fixed point of the renormalization group transformation with the zero of the partition function makes boundary contributions to the rate function on par with the bulk, to the extent of even annulling DQPT. For the one-dimensional case, the DQPTs are between two paramagnetic phases described by two different stable (i.e., attractive) fixed points. The transitions are first-order and are characterized by a periodic cycle of order 2.

For the two-dimensional models, we find alternating symmetry-breaking and restoring transitions between the para and ferro phases. The transitions are first-order, described by RG fixed points related by time-reversibility. To be noted here that the fixed point description for the first-order transitions are consistent with the discontinuous fixed points known for equilibrium phase transitions.

We may contrast the DQPT results with the thermal problem. One-dimensional Potts chain does not undergo any thermal phase transition, while, in two dimensions, there is a symmetry-breaking critical point (Curie point).

It has not escaped our notice that the first-order dynamic quantum phase transitions we observed in the

Potts system of discrete symmetry-breaking immediately suggests the possibility of interfaces separating the two coexisting phases. The nature of the interface in the quantum system remains to be elucidated.

Even for approximate real space RG for the Boltzmann factor, the transformation for y can be represented in terms of rational functions, and then the theory used here can be applicable. The complex dynamics formulation can be extended to many other systems including models in higher (> 2) dimensions, and also for more than one variables.

ACKNOWLEDGMENTS

The author thanks Jaya Maji for discussions on python and mathematica programs used in this paper. The author thanks Oleg Evnin and other organizers of the ‘5th Bangkok Workshop on Discrete Geometry, Dynamics and Statistics’, January 2023, at the physics department of Chulalongkorn University, Bangkok [55], where some of the results of this paper were presented.

Appendix A: RG equations

Some details of the RG procedure of Sec. IV are given here. The RG steps are indicated schematically in Fig. 9.

Note that a bond with two Potts spin in the same state has a weight of $y = e^{\beta J}$, while a bond with two different spins has a weight of 1. The decimation process involves removing (by summing over) the spins at the red square sites within each pink ellipse, while keeping the spins at the blue disk sites fixed. The new lattice is obtained by joining the blue sites with bonds. These are Steps 1 and 2 of Sec. IV. The blue spins are now coupled by a renormalized interaction or a renormalized weight y' . See Fig. 9.

The renormalization procedure preserves the physical properties, such as the partition function. The renormalized Hamiltonian is similar to the original one upto an additive constant. The additive constant in energy is the multiplicative factor c in the RG steps. The two unknowns

y' and c are then determined by equating the partition functions.

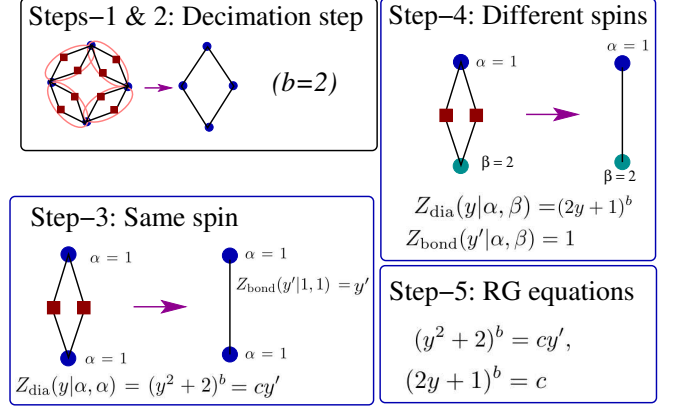


FIG. 9. The steps of RG transformation given in Sec. IV are shown schematically. The decimation is done by summing over the spins at the red square sites.

Appendix B: Recursion relations for the partition function

For small lattices, the Loschmidt amplitudes can be computed by constructing the recursion relations as the lattice is built up. By using the permutation symmetry of the spin orientations, the relations are written as

$$Z_n(y|\alpha, \alpha) = [Z_{n-1}(y|\alpha, \alpha)^2 + (q-1)Z_{n-1}(y|\alpha, \beta)^2]^b, (\beta \neq \alpha), \quad (\text{B1a})$$

$$Z_n(y|\alpha, \beta) = [2Z_{n-1}(y|\alpha, \alpha)Z_{n-1}(y|\alpha, \beta) + Z_{n-1}(y|\alpha, \gamma)Z_{n-1}(y|\gamma, \beta)]^b, (\beta \neq \alpha, \gamma \neq \alpha, \gamma \neq \beta), \quad (\text{B1b})$$

$$Z_n(y) = qZ_n(y|\alpha, \alpha) + q(q-1)Z_n(y|\alpha, \beta), \text{ any } \alpha \neq \beta. \quad (\text{B1c})$$

Appendix C: Periodic orbits for the Potts chain

For the one dimensional chain, there are no unstable fixed points, except the point at infinity. However, the Julia set contains many periodic orbits. The orbits of periodicity 2 to 5 are listed in Table II.

period	points (η) : $z = -0.5 + i\eta$	λ
2	$\pm \sin 2\pi/3$	2^2
3	$P_3 = \{-3.11478, -1.19621, 0.342365\},$ $-P_3$	2^3
4	$P_{4,1} = \{-7.05695, -3.36906, -1.35061, 0.157656\},$ $-P_{4,1},$ $P_{4,2} = \{-2.06457, -0.48738, 2.06457, 0.48738\},$	2^4
5	$P_{5,1} = \{-14.7507, -7.29908, -3.49541, -1.42586, +0.0760714\},$ $-P_{5,1},$ $-P_{5,2} = \{-1.16109, 0.388377, -2.70248, -0.934957, 0.735785\},$ $P_{5,3} = \{-0.555539, 1.74729, 0.229792, -4.78085, -2.15511\},$ $-P_{5,3}$	2^5

TABLE II. For the one-dimensional Potts model, the periodic orbits and their multipliers. The points are on the line $z = -0.5 + i\eta$, and only the η values are tabulated.

Appendix D: Julia set for the $b = 2$ Potts model

The Julia set for the $b = 2$ case is shown in Fig. 10. The unstable fixed point $y^* = 4$ of $R_2(y)$ from Eq. (40) belongs to the set, as do the preimages $y = 0, -2$ such that $R_2(y) = 4$. The color code in Fig.7 is based on the number of iterations needed for convergence.

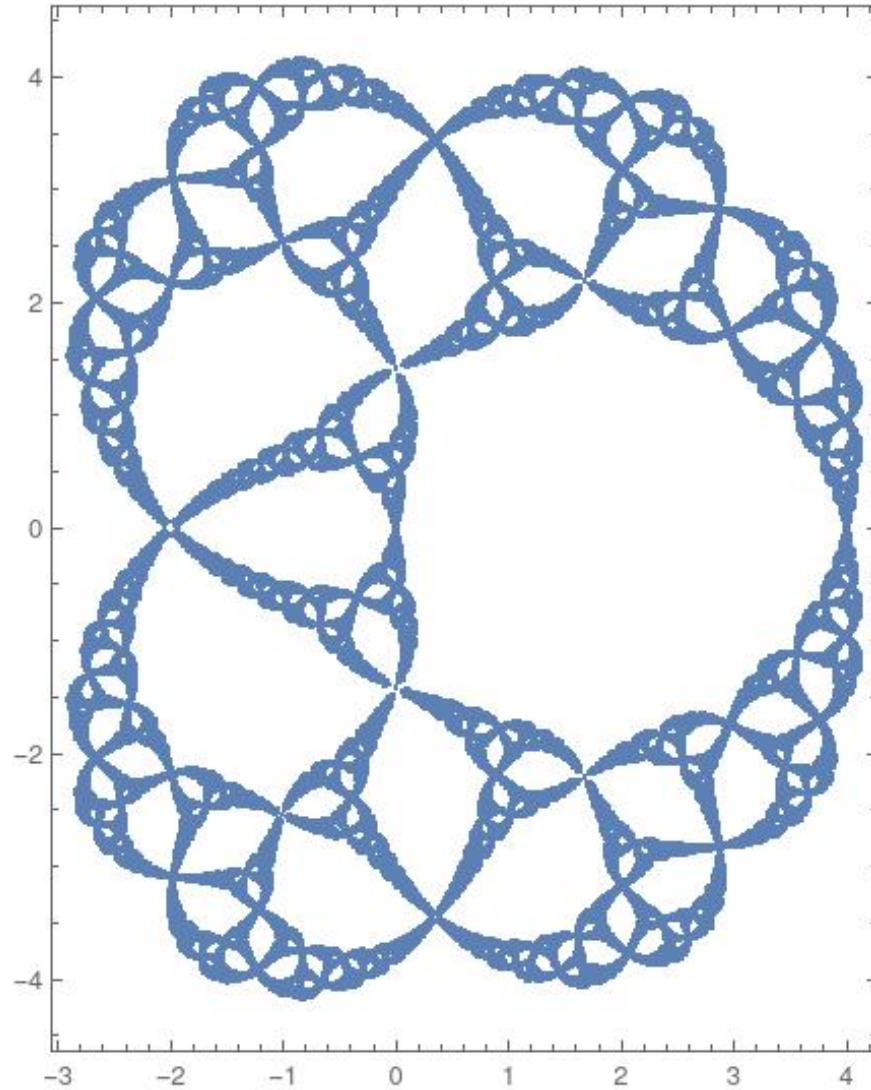


FIG. 10. The Julia set for the 3-state Potts model on the $b = 2$ diamond hierarchical lattice, obtained from MATHEMATICA [56].

- [1] M. Heyl, *Rept Prog. Phys.* **81**, 054001 (2018) and references therein.
- [2] A Khatun and S. M. Bhattacharjee, *Phys. Rev. Lett.* **123**, 160603 (2019).
- [3] A. Polkovnikov, K. Sengupta, A. Silva, and M. Vengalattore, *Rev. Mod. Phys.* **83**, 863 (2011).
- [4] P. Titum and M. F. Maghrebi, *Phys. Rev. Lett.* **125**, 040602 (2020).
- [5] S. Paul, P. Titum, M. F. Maghrebi, <https://doi.org/10.48550/arXiv.2202.04654>
- [6] M. Heyl, A. Polkovnikov, and S. Kehrein, *Phys. Rev. Lett.* **110**, 135704 (2013).
- [7] M. Heyl, *Phys. Rev. Lett.* **115**, 140602 (2015).
- [8] F. Andraschko and J. Sirker, *Phys. Rev. B* **89**, 125120 (2014).
- [9] D. Mondal and T. Nag, *Phys Rev B* **107**, 184311 (2023).
- [10] C. Karrasch and D. Schuricht, *Phys. Rev. B* **95**, 075143 (2017).
- [11] J-C Tang, W-L You, M-J Hwang, and G. Sun, *Phys. Rev. B* **107**, 134303 (2023).
- [12] A. A. Zvyagin, *Low Temp. Phys.* **42**, 971 (2016), and references therein.
- [13] B. Pozsgay, *J. Stat. Mech.*, **P10028** (2013).
- [14] P. Jurcevic, *et al*, *Phys. Rev. Lett.*, **119**, 080501 (2017).
- [15] N. Fläschner, *et al*, *Nature Physics*, **14**, 265 (2018).
- [16] R. Jafari and A. Akbari, *Phys. Rev. A* **103**, 012204 (2021).
- [17] S. Zamani, R. Jafari and A. Langari, *Phys. Rev. B* **102**, 144306 (2020).
- [18] M. Sadrzadeh, R. Jafari, and A. Langari, *Phys. Rev. B* **103**, 144305 (2021).
- [19] T. Masłowski, N. Sedlmayr - *Phys. Rev. B* **101**, 014301 (2020).
- [20] C. Rylands, E. A. Yuzbashyan, V. Gurarie, A. Zabalo, V. Galitski, *Annals of Physics* **435**, 168554 (2021).
- [21] G. Sun and B. B. Wei, *Phys. Rev. B* **102**, 094302 (2020).
- [22] D. Dolgitz, D. Zeng, Y. Chen, *Optics Express* **29**, 23988 (2021).
- [23] K. Cao, M. Zhong, and P. Tong, *J. Phys. A: Math. Theor.* **55**, 365001 (2022).
- [24] C. Ding, *Phys. Rev. B* **102**, 060409(R) (2020).
- [25] T. Tian, *et. al.*, *Phys. Rev. Lett.* **124**, 043001 (2020).
- [26] T. Hashizume, Ian P. McCulloch, and J. C. Halimeh *Phys. Rev. Research* **4**, 013250 (2022).
- [27] S. Porta, F. Cavaliere, M. Sasseti, and N. T. Ziani, *Scientific Reports* **10**, 12766 (2020).
- [28] More properly, the transition time is the time around which there is no Taylor series expansion in t of any relevant quantity like $\ln P(t)$.
- [29] S. R. S. Varadhan, *Ann. Prob.* **36**, 397 (2008).
- [30] K. Huang, *Statistical Mechanics*, 2nd Edition, Wiley 1987.
- [31] M. E. Fisher, “*The Nature of Critical Points*”, in *Lectures Theoretical Physics*, Vol VII C, Univ of Colorado Press, Boulder, 1965.
- [32] S. M. Bhattacharjee, *Critical Phenomena: An Introduction from a Modern Perspective*, in “*Field Theories in Condensed Matter Physics*”, Ed. by Sumathi Rao (Imprint: CRC Press, 2019).
- [33] F. Y. Wu, *Rev. Mod. Phys.* **54**, 235 (1982).
- [34] I. Affleck, M. Oshikawa and H. Saleur, *J. Phys. A: Math. Gen.* **31**, 5827 (1998).
- [35] Y-W. Dai, S. Y. Cho, M. T. Batchelor, and H-Q. Zhou *Phys. Rev. E* **89**, 062142 (2014).
- [36] N. Chepiga, *SciPost Phys. Core* **5**, 031 (2022).
- [37] R. B. Griffiths, and M. Kaufman, *Phys. Rev. B* **26**, 5022 (1982).
- [38] B. Derrida, L. De Seze, and C. Itzykson, *C.*, *J. Stat. Phys.* **33**, 559-569, 1983.
- [39] K. Akin and A. Nihat Berker, *Phys. Rev. E* **106**, 014151 (2022).
- [40] John W. Milnor, *Dynamics in One Complex Variable* (AM-160), 3rd Edition, (Princeton U Press, Princeton, 2006)
- [41] A. F. Beardon, *Iteration of rational functions*, (Springer-Verlag New York Inc., 2000).
- [42] L. Carleson and T. W. Gamelin, *Complex Dynamics* (Springer, 2011).
- [43] The diamond motif is not the only possibility. One may consider many other possible motifs [37].
- [44] S. M. Bhattacharjee, “What is dimension?”, in “*Topology and condensed matter physics*”, S. M. Bhattacharjee, Mahan Mj, A. Bandyopadhyay (Eds.), Springer, 2017.
- [45] Iterated maps are also denoted by R^n for the n th iterate.
- [46] If required, the distance between two points z_1 and z_2 in the extended plane \hat{C} can be taken as the arc-distance on the Riemann sphere or the Euclidean distance of the chord in 3-d. A metric is useful for trajectories going to ∞ .
- [47] More formally, if, for a point z_0 , for every $\epsilon > 0$ we can find a $\delta > 0$ such that $|R^{(n)}(z_0) - R^{(n)}(z)| < \delta$, for all n , implies $|z - z_0| < \epsilon$, then the trajectories are equicontinuous.
- [48] The q -state Potts model has a fixed point at $-(q - 1)$. In Eq. (11), given a value of α_j , only one state of the neighboring spin α_j contributes to the energy, while the remaining $q - 1$ states do not contribute. See Eq. (18c).
- [49] B. Nienhuis and M. Nauenberg, *Phys. Rev. Lett.* **35**, 477 (1975).
- [50] Note that as y may be complex, the Perron-Forbenius theorem is not applicable, unlike the real y case. The largest eigenvalue can be degenerate.
- [51] B. D. Craven, *J. Austra. Math. Soc.* **10**, 341 (1969).
- [52] S. M. Bhattacharjee and F. Seno, *J. Phys. A* **34**, 6375 (2001).
- [53] The Julia set is a compact and dense set of Hausdorff dimension ≈ 1.53 as estimated in D. Saupe, *Physica D* **28**, 358 (1987).
- [54] The preimages of $y = -2$, viz., $-0.3483106997490063... \pm 0.615889967883341...i$, and $0.348310699749006... \pm 3.444317092629529...i$, have similar geometrical or topological neighbourhoods.
- [55] <https://www.thaihep.phys.sc.chula.ac.th/BKK2023DSCR/>
- [56] Wolfram Research, Inc., *System Modeler*, Version 13.2, Champaign, IL (2023).